

## ON THE PERISTALTIC TRANSPORT OF A MICROPOLAR FLUID

K. N. D e y<sup>(1)</sup>, S. P o r i a<sup>(2)</sup>, H. P. M a z u m d a r<sup>(3)</sup>

<sup>(1)</sup>Department of Mathematics  
Maharaja Monindra Chandra College,  
Calcutta-700003, India.

<sup>(2)</sup>Department of Mathematics  
Midnapore College, Midnapore,  
West Bengal, India.

<sup>(3)</sup>Physics and Applied Mathematics Unit  
Indian Statistical Institute,  
Calcutta-700035, India.

In this paper, we study some characteristics of the peristaltic motion of an incompressible micropolar fluid through a circular cylindrical tube. Many authors have investigated the peristaltic motion of non-Newtonian or viscoelastic fluid through a channel or tube due to the relevance of peristaltic action in both mechanical and physiological situations. For example, peristaltic mechanism may be involved in vasomotion of small blood vessels. Here the microstructural effects on the pressure rise, average flow and friction force are investigated.

### 1. INTRODUCTION

In recent years, the mechanism of peristaltic pumping i.e., the transport of a fluid by a wave of contraction and/or expansion propagating along the walls of a tube or channel has received much attention of the researchers because of its applications to some mechanical and physiological situations. For example, peristaltic motions are involved in the transport of spermatazoa in cervical canal, cilia transport through the ductus efferente of the male reproductive organ, functioning of ureter and expansion or contraction of small blood vessels. Several authors have contributed to the peristaltic transport of Newtonian and non-Newtonian fluid through tubes or channels. In reference [1], peristaltic transport of inertia free, Newtonian flows driven by sinusoidal transversal waves of small amplitude has been studied. The closed form solutions for peristaltic waves of long wavelength and arbitrary amplitude are obtained in paper [2]. While, the effects of fluid inertia and wall curvature and alignment on peristaltic flow patterns and pumping flow characteristics have been investigated in paper [3]. Some

authors [4, 5, 6] have studied the shear thinning and shear thickening effects on the peristaltic transport of non-Newtonian fluids. In paper [7], the peristaltic transport of a power-law fluid has been studied in reference to the ductus efferentes of the reproductive tract. The peristaltic transport mechanism, in the case when viscosity of transported fluid is shear-dependent and direction of mean flow can oppose the direction of wave propagation in presence of a zero or favourable mean pressure gradient has been analyzed in reference [8]. The vasomotion of the small blood vessels, considering blood as a viscoelastic fluid has been discussed in paper [9].

In the present model, we treat blood as a suspension of particulate matter in a microscopically continuous media. The theory of micro-fluids, which are applied to flow in rheologically complex fluids, such as liquid crystals, polymeric suspensions and animal blood was developed in reference [10]. A subclass of these fluids which can support couple stresses and body couples and exhibit microrotational effects and microrotational inertia are termed micropolar fluids [11]. In effect, we investigate the peristaltic transport of a micropolar fluid through a circular tube under long wavelength approximations. Microstructural effects on the pressure rise, flow rate and friction force are determined.

## 2. ANALYSIS OF THE PROBLEM

We consider here the peristaltic transport of a simple incompressible micropolar fluid through an axially symmetric circular tube (Fig. 1). Since the walls of the tube are executing sinusoidal wave motion due to peristalsis, the geometry of the tube wall is given by

$$(2.1) \quad \begin{aligned} h(X, t) &= a' + b' \sin \left\{ \frac{2\pi}{\lambda} (X - ct) \right\} \\ &= a' \left[ 1 + \epsilon \sin \frac{2\pi}{\lambda} (X - ct) \right]. \end{aligned}$$

Here  $a'$  is the mean radius of the tube and  $b'$  is the amplitude of the wave,  $\epsilon = a'/b' (< 1)$  is the dimensionless amplitude of the wave.  $a'(1 + \epsilon)$  and  $a'(1 - \epsilon)$  are, respectively the maximum and minimum disturbed radii,  $\lambda$  is the wavelength,  $c$  the phase velocity,  $t$  is the time and  $X$  is the axial coordinate. The wavelength  $\lambda$  is assumed to be much larger than the radius  $a'$  of the tube (i.e.,  $a'/\lambda \ll 1$ ). Now it is convenient to use the moving coordinate system  $(r, x)$  travelling with the wave so that  $r = R$ ,  $x = X - ct$  where  $(R, X)$  is the stationary coordinate system. Let  $(U, V)$  and  $(u, v)$  be the velocity components, respectively in the stationary and moving coordinate system, then

$$(2.2) \quad U = u, \quad V = v + c.$$

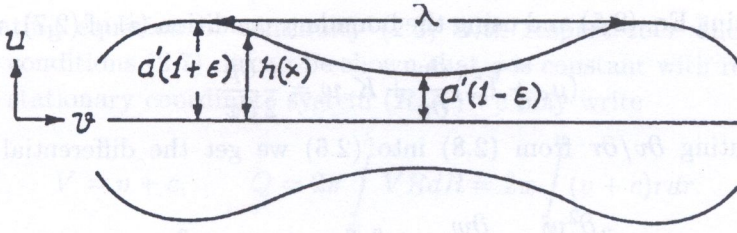


FIG. 1. Tube geometry.

Now, using very long wavelength approximation and neglecting inertial terms, the equations of continuity and momentum in cylindrical polar coordinates, are given by (following [11])

$$(2.3) \quad \frac{\partial(ru)}{\partial r} + \frac{\partial(rv)}{\partial x} = 0,$$

$$(2.4) \quad \frac{\partial p}{\partial r} = 0,$$

$$(2.5) \quad (\mu_v + K_v) \frac{1}{r} \frac{\partial}{\partial r} \left( r \frac{\partial v}{\partial r} \right) + \frac{K_v}{r} \frac{\partial(rw)}{\partial r} = \frac{\partial p}{\partial x},$$

$$(2.6) \quad \nu_v \frac{\partial}{\partial r} \left[ \frac{1}{r} \frac{\partial(rw)}{\partial r} \right] - K_v \frac{\partial v}{\partial r} - 2K_v w = 0,$$

where  $\mu_v$  is the viscosity of the fluid,  $w$  is the suspending particle rotation,  $K_v$  is the relative rotational viscosity and  $\nu_v$  is the viscosity gradient of the total rotation.

The boundary conditions are chosen, as

$$(2.7) \quad \begin{aligned} (i) \quad & \frac{\partial v}{\partial r} = 0 && \text{at } r = 0, \\ (ii) \quad & u = 0 && \text{at } r = 0, \\ (iii) \quad & w = 0 && \text{at } r = 0, \\ (iv) \quad & v = -c && \text{at } r = h, \\ (v) \quad & u = \frac{\partial h}{\partial t} = v|_{r=h} \cdot \frac{\partial h}{\partial x} && \text{at } r = h, \\ \text{and } (vi) \quad & \frac{1}{r} \frac{\partial(rw)}{\partial r} = 0 && \text{at } r = h. \end{aligned}$$

From Eq. (2.4) it is seen that  $p$  is independent of  $r$  and we may treat the pressure  $p$  as a function of  $x$  only,  $p = p(x)$ .

Integrating Eq. (2.5) and using the boundary condition (i) of (2.7), we obtain,

$$(2.8) \quad (\mu_v + K_v) \frac{\partial v}{\partial r} + K_v w = \frac{r}{2} \frac{\partial p}{\partial x}.$$

Substituting  $\partial v/\partial r$  from (2.8) into (2.6) we get the differential equation for  $w$  as

$$(2.9) \quad r^2 \frac{\partial^2 w}{\partial r^2} + r \frac{\partial w}{\partial r} - (\beta^2 r^2 + 1)w = Ar^3.$$

where

$$(2.10) \quad \beta^2 = \frac{(K_v + 2\mu_v)K_v}{(\mu_v + K_v)\nu_v}, \quad A = \frac{K_v}{2\nu_v} \frac{1}{(\mu_v + K_v)} \frac{\partial p}{\partial x}.$$

On using the boundary conditions (iii) and (vi) of (2.7), we obtain the solution of the differential Eq. (2.9) as

$$(2.11) \quad w = -\frac{1}{2(K_v + 2\mu_v)} \frac{\partial p}{\partial x} \left[ r - \frac{2}{\beta} \frac{I_1(\beta r)}{I_0(\beta h)} \right]$$

where  $\beta$  is given in (2.10) and  $I_n(x)$  is the modified Bessel function of order  $n$ . Putting the value of  $w$  from (2.11) in (2.8) we get the differential equation for  $v$  as

$$(2.12) \quad (\mu_v + K_v) \frac{\partial v}{\partial r} - \frac{K_v}{2(K_v + 2\mu_v)} \frac{\partial p}{\partial x} \left[ r - \frac{2}{\beta} \frac{I_1(\beta r)}{I_0(\beta h)} \right] = \frac{r}{2} \frac{\partial p}{\partial x}.$$

Integrating Eq. (2.12) and using the boundary condition (i) of (2.7) we obtain

$$(2.13) \quad v = -c - \frac{1}{4(\mu_v + K_v)} \frac{\partial p}{\partial x} \left[ (h^2 - r^2) \frac{2(\mu_v + K_v)}{(K_v + 2\mu_v)} + \frac{4K_v}{(K_v + 2\mu_v)} \frac{1}{\beta^2} \left\{ \frac{I_0(\beta r) - I_0(\beta h)}{I_0(\beta h)} \right\} \right].$$

With the assumption that the observer is moving with velocity  $c$ , the flow rate  $q$  in the moving coordinate system is given by

$$(2.14) \quad q = 2\pi \int_0^h r v dr.$$

Substituting the value of  $v$  from (2.13) in (2.14) and performing integration, we obtain

$$(2.15) \quad q = -\pi c h^2 - \frac{\pi}{4(\mu_v + K_v)} \frac{\partial p}{\partial x} \left[ \frac{\mu_v + K_v}{K_v + 2\mu_v} h^4 + \frac{8K_v}{K_v + 2\mu_v} \frac{h}{\beta^2 I_0(\beta h)} \cdot \left\{ \frac{1}{\beta} I_1(\beta h) - \frac{h}{2} I_0(\beta h) \right\} \right].$$

Integrating equation of continuity (2.3) with respect to  $r$  and using the boundary conditions (2.7), it can be shown that  $q$  is constant with respect to  $x$ .

In the stationary coordinate system  $(R, X)$  we may write

$$V = v + c, \quad Q = 2\pi \int_0^h VRdR = 2\pi \int_0^h (v + c)rdr.$$

Thus

$$(2.16) \quad Q = q + \pi ch^2.$$

Taking the average over one period,

$$(2.17) \quad \bar{Q} = \frac{1}{\lambda} \int_0^\lambda Q dx = \frac{1}{\lambda} \int_0^\lambda (q + \pi ch^2) dx.$$

Substituting  $h = a' \left[ 1 + \epsilon \sin \frac{2\pi}{\lambda} x \right]$  in (2.17) we obtain

$$(2.18) \quad \bar{Q} = q + \pi ca'^3 \left( 1 + \frac{\epsilon^2}{2} \right).$$

The pressure drop  $\Delta p = p(0) - p(\lambda)$  across one wavelength is the same whether it is measured in the fixed or moving coordinate system, given by

$$(2.19) \quad \Delta p = - \int_0^\lambda \frac{\partial p}{\partial x} dx.$$

Here  $\partial p/\partial x$  can be determined from Eq. (2.15). On using Eq. (2.19) we determine pressure drop as

$$(2.20) \quad \Delta p = \frac{4(\mu_v + K_v)}{\pi} \int_0^\lambda \frac{\bar{Q} - \pi ca'^2 \left( 1 + \frac{\epsilon^2}{2} \right) + \pi ch^2}{ah^4 + 8b \frac{h}{\beta^2 I_0(\beta h)} \left\{ \frac{1}{\beta} I_1(\beta h) - \frac{h}{2} I_0(\beta h) \right\}} dx$$

where

$$(2.21) \quad a = \frac{\mu_v + K_v}{K_v + 2\mu_v}, \quad b = \frac{K_v}{K_v + 2\mu_v}, \quad \beta^2 = \frac{(K_v + 2\mu_v)K_v}{(\mu_v + K_v)} \nu_v$$

The frictional force  $F$  at the wall in the stationary coordinate system which is the same as in the moving system across one wavelength is given by

$$(2.22) \quad F = - \int_0^\lambda \pi h^2 \frac{dp}{dx} dx.$$

On using (2.15), (2.16), (2.18) and (2.22) we obtain easily

$$(2.23) \quad F = 4(\mu_v + K_v) \int_0^\lambda \frac{\bar{Q} - \pi ca'^2 \left(1 + \frac{\epsilon^2}{2}\right) + \pi ch^2}{ah^4 + 8b \frac{h}{\beta^2 I_0(\beta h)} \left\{ \frac{1}{\beta} I_1(\beta h) - \frac{h}{2} I_0(\beta h) \right\}} dx$$

where  $a, b, \beta^2$  are given by (2.21).

### 3. NUMERICAL RESULTS AND DISCUSSION

For numerical computations we use the values for  $\mu_v$ ,  $K_v$  and  $\nu_v$  (following [12] and [13]) as  $\mu_v = 0.8, 1, 1.4$  c.p.,  $K_v = 0.82, 0.98, 1.14$  c.p. and  $\nu_v = 12 \times 10^{-8}$  g. cm/s. The values of  $a', c$  and  $\epsilon$  are chosen as (see references [8] and [14])  $a' = 0.9$  cm,  $c = 0, 50, 100, 150$  cm s $^{-1}$  and  $\epsilon = 0, 0.1, 0.2$ .

We compute the flow flux, pressure rise and friction force from Eqs. (2.15), (2.20) and (2.23). The integrations in (2.20) and (2.23) are done numerically.

The variation of pressure rise with  $\bar{Q}$  are illustrated in Figs. 2 and 3. In Fig. 2, the profiles are shown for different  $\mu_v$ , e.g.  $\mu_v = 0.8, 1, 1.4$ . Here the value of  $K_v$  is taken as  $K_v = 0.98$ . It can be seen from Fig. 2 that pressure rise decreases as  $\bar{Q}$  increases and the maximum pressure rise occurs at zero flow rate. It is also

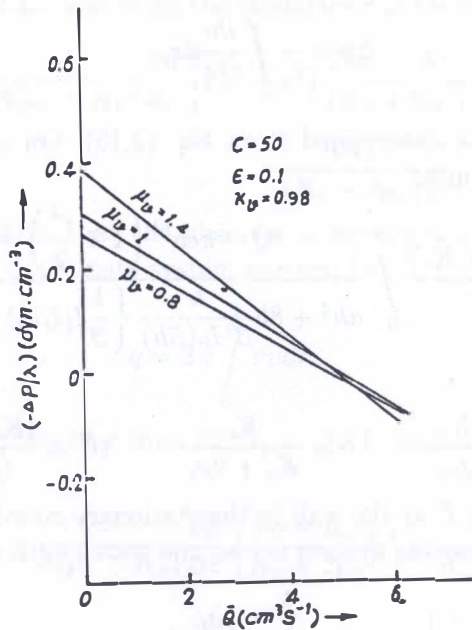


FIG. 2. Variation of  $-\Delta p/\lambda$  with  $\bar{Q}$  for different  $\mu_v$ .

seen that zero pressure difference across a wavelength is achieved around  $\bar{Q} = 5$ . It is also observed that the pressure rise with  $\bar{Q}$  is shown for different  $K_v$ , e.g.  $K_v = 0, 0.82, 1.14$ . The value of  $\mu_v$  is taken as  $\mu_v = 1$ . It seen in this figure that the pressure increases with the increase of rotational viscosity  $K_v$ . Thus the microstructural effect increases the pressure for a given value of  $\bar{Q}$ .

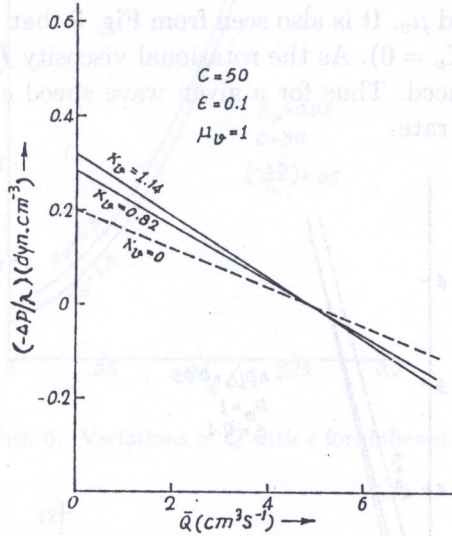


FIG. 3. Variations of  $-\Delta p/\lambda$  with  $\bar{Q}$  for different  $K_v$ .

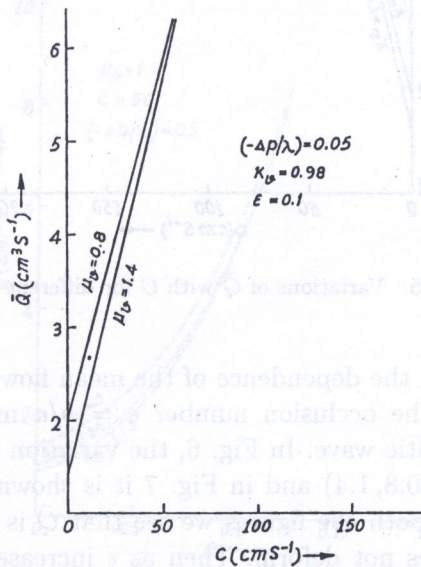


FIG. 4. Variations of  $\bar{Q}$  with  $C$  for different  $\mu_v$ .

The variations of flow rate with wave speed  $c$  are illustrated in Fig. 4 and Fig. 5. In both the figures the value of  $-\Delta p/\lambda$  is taken to be 0.05. In Fig. 4 the profiles are shown for different  $\mu_v$ , e.g.  $\mu_v = 0.8, 1.4$  with fixed  $k_v(0.98)$  and they are shown for different  $K_v$ , e.g.  $K_v = 0, 0.82, 1.14$  with fixed  $\mu_v(1.0)$  in Fig. 5. For each profile it is seen that  $\bar{Q}$  is minimum at  $c = 0$ . As the wave speed is increased from 0, it is expected that the mean flow rate will increase, as it does in Fig. 4 and Fig. 5. In Fig. 4, it is seen that the flow rate decreases with increasing the viscosity of the fluid  $\mu_v$ . It is also seen from Fig. 5 that the flow rate is larger for Newtonian fluid ( $K_v = 0$ ). As the rotational viscosity  $K_v$  increases, the flow rate is seen to be reduced. Thus for a given wave speed  $c$ , the microstructural effect reduces the flow rate.

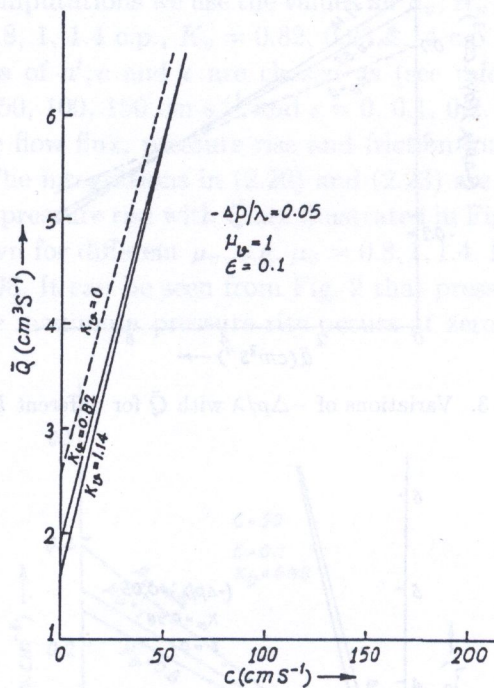


FIG. 5. Variations of  $\bar{Q}$  with  $C$  for different  $K_v$ .

In Fig. 6 and Fig. 7, the dependence of the mean flow on occlusion is shown when  $\Delta p/\lambda = 0.05$ . The occlusion number  $\epsilon = b/a$  measures the degree of occlusion of the peristaltic wave. In Fig. 6, the variation of  $\bar{Q}$  on  $\epsilon$  is shown for different  $\mu_v$  (e.g.  $\mu_v = 0.8, 1.4$ ) and in Fig. 7 it is shown for different  $K_v$  (e.g.  $K_v = 0, 0.98, 1.14$ ). In both the figures we see that  $\bar{Q}$  is minimum when  $\epsilon = 0$  i.e., when the tube does not deform. Then as  $\epsilon$  increases, the mean flow rate increases steadily towards its positive limiting value at full occlusion.

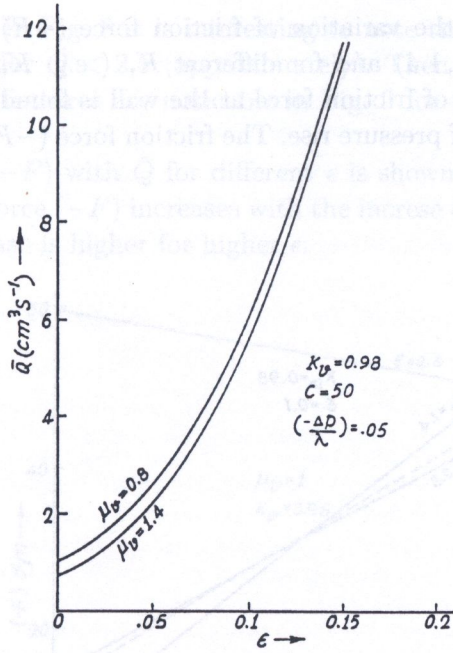


FIG. 6. Variations of  $\bar{Q}$  with  $\epsilon$  for different  $\mu_v$ .

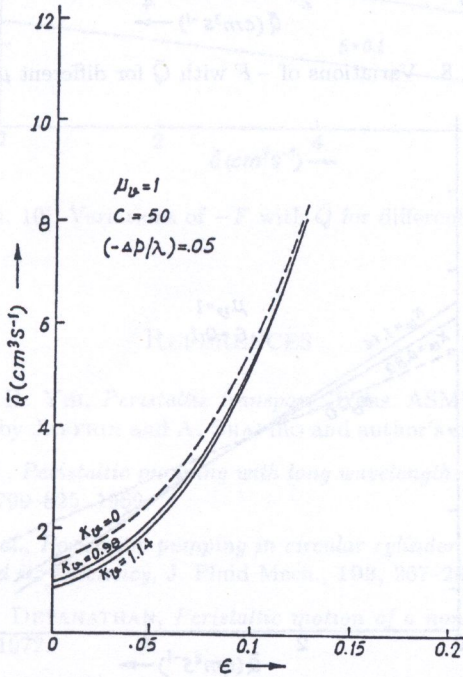


FIG. 7. Variations of  $\bar{Q}$  with  $\epsilon$  for different  $K_v$ .

Figures 8 and 9 show the variation of friction force ( $-F$ ) with  $\bar{Q}$  for different  $\mu_v$  (e.g.  $\mu_v = 0.8, 1, 1.4$ ) and for different  $K_v$  (e.g.  $K_v = 0, 0.82, 1.14$ ) respectively. The variation of friction force at the wall is found to be similar to that observed in the case of pressure rise. The friction force ( $-F$ ) decreases with

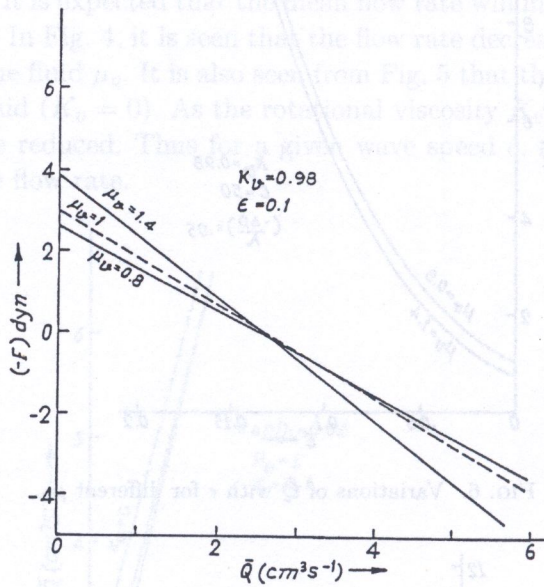


FIG. 8. Variations of  $-F$  with  $\bar{Q}$  for different  $\mu_v$ .

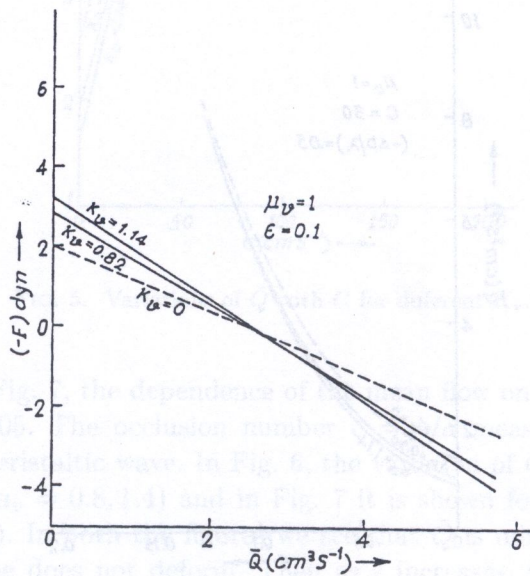


FIG. 9. Variations of  $-F$  with  $\bar{Q}$  for different  $K_v$ .

the increase of  $\bar{Q}$ . In Fig. 8 it is interesting to note that the friction force ( $-F$ ) is greater for  $\mu_v$  for  $\bar{Q} < 2.5$  (approximately). Then for  $\bar{Q} > 2.5$ , the effect is reversed. Similar features are noticeable in Fig. 9 for the variation of rotational viscosity  $K_v$ .

Variation of ( $-F$ ) with  $\bar{Q}$  for different  $\epsilon$  is shown in Fig. 10. It is observed that the friction force ( $-F$ ) increases with the increase of amplitude of the wave  $\epsilon$ . The rate of increase is higher for higher  $\epsilon$ .

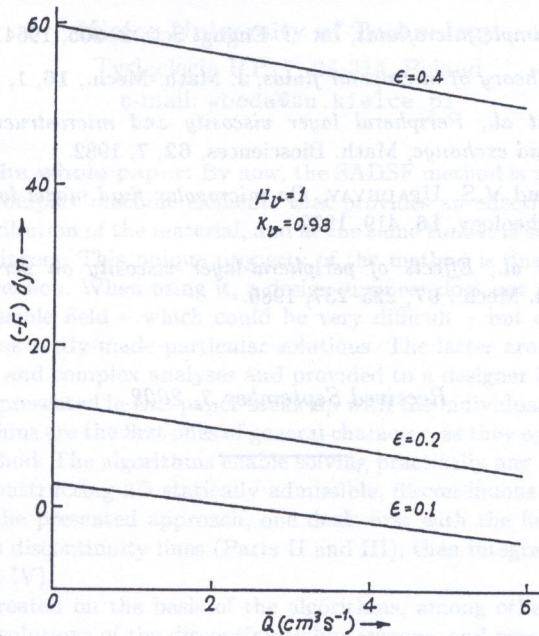


FIG. 10. Variations of  $-F$  with  $\bar{Q}$  for different  $\epsilon$ .

#### REFERENCES

1. Y.C. FUNG, and C.H. YIH, *Peristaltic transport*, Trans. ASME J: J. Appl. Mech., **35**, 669-675. Discussion by JAFFRIN and A. SHAPIRO and author's closure, **36**, 379-382, 1968.
2. A.H. SHAPIRO, *et al.*, *Peristaltic pumping with long wavelengths at low Reynolds number*, J. Fluid Mech., **37**, 799-825, 1969.
3. S. TAKABATAKE, *et al.*, *Peristaltic pumping in circular cylinder tubes: A numerical study of fluid transport and its efficiency*, J. Fluid Mech., **193**, 267-283, 1988.
4. K.K. RAJU, and R. DEVANATHAN, *Peristaltic motion of a non-Newtonian fluid*, Rheol. Acta., **11**, 170-178, 1972.
5. B.F. PICOLOGLOU, *et al.*, *Biorheological aspects of colonic activity. Part I. Theoretical considerations*, Biorheology, **10**, 431-440, 1973.

6. J.B. SHUKLA, and S.P. GUPTA, *Peristaltic transport of a power-law fluid with variable consistency*, Trans. ASMEK: J. Biomech. Engng., **104**, 182-186, 1982.
7. L.M. SRIVASTAVA and V.P. SRIVASTAVA, *Peristaltic transport of a power-law fluid : application to the ductus efferentes of reproductive tract*, Rheological Acta, **27**, 428-433, 1988.
8. M. PROVOST ALDEN, and W.H. SCHWARZ, *A theoretical study of viscous effects in peristaltic pumping*, J. Fluid Mech., **279**, 177-195, 1994.
9. G. BOHME, and R. FRIEDRICH, *Peristaltic flow of viscoelastic liquid*, J. Fluid Mech., **128**, 109-122, 1983.
10. A.C. ERINGEN, *Simple microfluids*, Int. J. Engng. Sci., **2**, 205, 1964.
11. A.C. ERINGEN, *Theory of micropolar fluids*, J. Math. Mech., **16**, 1, 1966.
12. P.N. TANDON, et al., *Peripheral layer viscosity and microstructural effects on the capillary-tissue fluid exchange*, Math. Biosciences, **62**, 7, 1982.
13. P. CHATURANI, and V.S. UPADHYAY, *On micropolar fluid model for blood flow through narrow tubes*, Biorheology, **16**, 419, 1979.
14. J.B. SHUKLA, et al., *Effects of peripheral-layer viscosity on peristaltic transport of a biofluid*, J. Fluid. Mech., **97**, 225-237, 1980.

*Received September 3, 2002.*